



## Pt-catalyzed ozonation of aqueous phenol solution using high-gravity rotating packed bed

Chia-Chi Chang<sup>a</sup>, Chun-Yu Chiu<sup>b</sup>, Ching-Yuan Chang<sup>a,\*</sup>, Chiung-Fen Chang<sup>c</sup>, Yi-Hung Chen<sup>d</sup>, Dar-Ren Ji<sup>a</sup>, Jyi-Yeong Tseng<sup>a</sup>, Yue-Hwa Yu<sup>a</sup>

<sup>a</sup> Graduate Institute of Environmental Engineering, National Taiwan University, Taipei 106, Taiwan

<sup>b</sup> Department of Cosmetic Science and Application, Lan-Yang Institute of Technology, I-Lan 261, Taiwan

<sup>c</sup> Department of Environmental Science and Engineering, Tunghai University, Taichung 407, Taiwan

<sup>d</sup> Department of Chemical Engineering and Biotechnology, National Taipei University of Technology, Taipei 106, Taiwan

### ARTICLE INFO

#### Article history:

Received 1 December 2008

Received in revised form 12 February 2009

Accepted 12 February 2009

Available online 21 March 2009

#### Keywords:

Ozone

Catalyst

High-gravity rotating packed

Phenol

### ABSTRACT

In this study, a high-gravity rotating packed bed (HGRPB or HG) was used as a catalytic ozonation (Cat-OZ) reactor to decompose phenol. The operation of HGRPB system was carried out in a semi-batch apparatus which combines two major parts, namely the rotating packed bed (RPB) and photo-reactor (PR). The high rotating speed of RPB can give a high volumetric gas–liquid mass transfer coefficient with one or two orders of magnitude higher than those in the conventional packed beds. The platinum-containing catalyst (Dash 220N, Pt/ $\gamma$ -Al<sub>2</sub>O<sub>3</sub>) and activated alumina ( $\gamma$ -Al<sub>2</sub>O<sub>3</sub>) were packed in the RPB respectively to adsorb molecular ozone and the target pollutant of phenol on the surface to catalyze the oxidation of phenol. An ultra violet (UV) lamp (applicable wavelength  $\lambda = 200$ –280 nm) was installed in the PR to enhance the self-decomposition of molecular ozone in water to form high reactive radical species. Different combinations of advanced oxidation processes (AOPs) with the HGRPB for the degradation of phenol were tested. These included high-gravity OZ (HG-OZ), HG catalytic OZ (HG-Cat-OZ), HG photolysis OZ (HG-UV-OZ) and HG-Cat-OZ with UV (HG-Cat-UV-OZ). The decomposition efficiency of total organic compound ( $\eta_{\text{TOC}}$ ) of HG-UV-OZ with power of UV ( $P_{\text{UV}}$ ) of 16 W is 54% at applied dosage of ozone per volume sample  $m_{\text{A,in}} = 1200 \text{ mg L}^{-1}$  (reaction time  $t = 20 \text{ min}$ ), while that of HG-OZ without the UV irradiation is 24%. After 80 min oxidation ( $m_{\text{A,in}} = 4800 \text{ mg L}^{-1}$ ), the  $\eta_{\text{TOC}}$  of HG-UV-OZ is as high as 94% compared to 82% of HG-OZ process. The values of  $\eta_{\text{TOC}}$  for HG-Cat-OZ process with  $m_{\text{S}} = 42 \text{ g}$  are 56% and 87% at  $m_{\text{A,in}} = 1200$  and  $4800 \text{ mg L}^{-1}$ , respectively. By increasing the catalyst mass to 77 g, the  $\eta_{\text{TOC}}$  for the HG-Cat-OZ process reaches 71% and 90% at  $m_{\text{A,in}} = 1200$  and  $4800 \text{ mg L}^{-1}$ , respectively. The introduction of Pt/ $\gamma$ -Al<sub>2</sub>O<sub>3</sub> as well as UV irradiation in the HG-OZ process can enhance the  $\eta_{\text{TOC}}$  of phenol significantly, while  $\gamma$ -Al<sub>2</sub>O<sub>3</sub> exhibits no significant effect on  $\eta_{\text{TOC}}$ . For the HG-Cat-UV-OZ process with  $m_{\text{S}} = 42 \text{ g}$ , the values of  $\eta_{\text{TOC}}$  are 60% and 94% at  $m_{\text{A,in}} = 1200$  and  $4800 \text{ mg L}^{-1}$ , respectively. Note that the decomposition of TOC via HG-UV-OZ is already vigorous. Thus, the enhancing effect of catalyst on  $\eta_{\text{TOC}}$  is minor.

© 2009 Elsevier B.V. All rights reserved.

### 1. Introduction

The ozone-based advanced oxidation processes (AOPs) such as sole ozonation (OZ), photolysis ozonation (UV-OZ) and catalytic ozonation (Cat-OZ) have been widely applied in water and wastewater treatment [1–7]. However, the decomposition of organic compounds in solution via OZ process is limited by gas–liquid mass transfer efficiency and its selective reactivity. The conventional ozonation reactors such as bubble column and completely stirred tank reactor (CSTR) are commonly used in sewage treatment plants. Although the gas/liquid mass transfer efficiencies of

these reactors can be enhanced via increasing the height and stirring speed ( $N_r$ ) of the respective reactors, but the use of catalyst in such reactors still encounters the packing problem. In order to further promote the decomposition efficiency of organics in ozonation processes, the catalysts of transition metals have been usually used for catalyzing the formation of more powerful radicals. For example, the heterogeneous catalysts of metal oxides or metals on supports are widely used for enhancing the activation of ozone [2]. The catalysts with metals such as Pt, Ru, Rh, Pd and Ag were reported to be effective for the decomposition of organic compounds in gaseous as well as aqueous phase ozonation. Platinum on the Al<sub>2</sub>O<sub>3</sub> surface is effective for the decomposition of O<sub>3</sub> in gaseous as well as aqueous phase [8,9]. The order of catalytic activity of metals supported on Al<sub>2</sub>O<sub>3</sub> was found to be: Pt > Pd > Ag > Ru ~ Rh ~ Ir > Ni > Cd > Mn > Fe > Cu > Zn ~ Zr [10]. The

\* Corresponding author. Tel.: +886 2 2363 8994; fax: +886 2 2363 8994.

E-mail address: [cychang3@ntu.edu.tw](mailto:cychang3@ntu.edu.tw) (C.-Y. Chang).

mechanism of the heterogeneous catalytic ozonation in water was explained by Legube and Vel Leitner [1]. Based on the mechanism, the Pt on the Dash 220N surface assists the generation of  $\bullet\text{OH}$  radicals. The organic molecules (phenol and intermediates) are adsorbed on the active site on Dash 220N surface and oxidized via an electron-transfer reaction. Then the organic radical species are desorbed from the Dash 220N and oxidized by  $\bullet\text{OH}$  radical or  $\text{O}_3$ .

In this study, a high-gravity rotating packed bed (HGRPB, HG or Hige) system was employed to decompose the phenol solution. The HGRPB was also used as a catalyst bed to house the catalysts as well as a gas–liquid contactor to enhance the mass transfer rate between the phases. The function of HGRPB can increase the interfacial area while decrease the mass transfer resistance between gas and liquid phases via decreasing the thickness of the liquid film and the size of the droplets [11]. The values of volumetric gas–liquid mass transfer coefficients achievable in HGRPB are one or two orders of magnitude higher than those in the conventional packed beds [12]. The use of HGRPB as an ozone mass transfer apparatus can improve the gas–liquid mass transfer efficiency and increase the oxidation ability of the OZ system. The advantages of combined HGRPB and OZ process were also noted by Chang et al. [13] in a study for the treatment of dimethyl phthalate solution.

In this work, the HGRPB was applied to the catalytic ozonation processes using Pt/ $\gamma\text{-Al}_2\text{O}_3$  and  $\gamma\text{-Al}_2\text{O}_3$ , respectively to decompose the organic compound of phenol in aqueous solution. System performances for the degradation of phenol via various AOPs using HGRPB were examined and compared. Different combinations of AOPs with HGRPB for the degradation of phenol were also tested. These included high-gravity OZ (HG-OZ), HG catalytic OZ (HG-Cat-OZ), HG photolysis OZ (HG-UV-OZ) and HG-Cat-OZ with UV (HG-Cat-UV-OZ).

## 2. Experimental

### 2.1. Chemicals

The phenol (Sigma–Aldrich Co., St. Louis, MO, USA) was subjected to de-ionized (DI) water to prepare the solution with the concentration ( $C_{\text{BLO}}$ ) of  $100\text{ mg L}^{-1}$ . The initial pH value of phenol solution was about 7.2. The effluent  $\text{O}_3$  absorbent solution of potassium iodine (KI) and the mobile phase of acetonitrile ( $\text{CH}_3\text{CN}$ ) for the high performance liquid chromatography (HPLC) used were analytical grade (Baker, Phillipsburg, NJ, USA). Ozone was decomposed to form radicals via a commercial platinum-containing catalyst (Pt/ $\gamma\text{-Al}_2\text{O}_3$ ) Dash 220N (N.E. Chemcat Co., Tokyo, Japan), which is a spherical catalyst in 3–4 mm diameter. The bulk density of Dash 220N is  $0.77\text{ g cm}^{-3}$ . The content of platinum in the alumina sphere is about 0.23 wt%.

### 2.2. Instrumentation

The HGRPB ozonation system (Fig. 1) was carried out via semi-batch operation. The experiments were performed with the volume ( $V_L$ ) of phenol solution of 1 L and total reaction time ( $t$ ) of 80 min. The HGRPB system has two major parts, namely the RPB and photo-reactor. The RPB consists of a packing chamber, a rotor and a stationary housing. The phenol solution flowed outward from the inner edge of the packing chamber subjected to the centrifugal force. On the other hand, gaseous ozone flowed inward countercurrently from the outer edge of the packed bed via the pressure-driving force. The spherical glass beads and Dash 220N catalyst were used as packing materials. The diameter of glass beads is about the same as that of Dash 220N. The RPB is 2 cm in high and 5.9 cm in diameter. In the experiments, the RPB was operated with rotating speed ( $N_r$ ) of 1500 rpm, which provided a gravita-

tional force of  $148.55\text{ g}$  ( $1455\text{ m s}^{-2}$ ). The phenol solution was fed to RPB by a peristaltic pump at  $462\text{ mL min}^{-1}$  recycle rate ( $Q_{\text{LR}}$ ) and contacted with gaseous ozone and catalysts in the bed.

The photo-reactor of the HGRPB system is made of Pyrex glass with the dimensions of diameter and height of 5 and 30 cm, respectively. A UV lamp (TUV-16W, Phillips, Tokyo, Japan) was placed at the center of the UV reactor and shielded by a quartz jacket. The UV irradiation was introduced to enhance the decomposition of ozone to form the  $\bullet\text{OH}$  radical. All the experiments were controlled at  $25^\circ\text{C}$  with water jacket around the reactor. The phenol solution was pumped and recycled continuously through a closed loop connected with monitors of pH value (TS-2, Suntex, Taipei, Taiwan), oxidation–reduction potential (ORP) (ORP-900C, Apogee, CA, USA) and dissolved ozone ( $\text{DO}_3$ ) (Model 3600, Orbisphere, Trasadingen, Switzerland). Liquid samples were taken from a sampling port for chemical analyses.

The ozone was generated from dried oxygen with purity of 99.99% via corona discharge using an ozone generator (Model LAB2B, Ozonia, Duebendorf, Switzerland). The ozone inlet flow rate ( $Q_G$ ) was controlled via a mass flow controller (MFC, Model 5850E, Brooks, Hatfield, PA, USA) at  $1\text{ L min}^{-1}$ . The inlet and outlet gaseous ozone concentrations were measured via a UV/visible spectrophotometer (UV mini-1240, Shimadzu, Kyoto, Japan) with the absorbance of ozone measured in a 2 mm flow-through quartz cell at the wavelength of 258 nm. An extinction coefficient of  $3000\text{ M}^{-1}\text{ s}^{-1}$  was used to convert absorbances into concentration units [14]. The inlet ozone concentration ( $C_{\text{AG},\text{in}}$ ) was controlled at  $60\text{ mg L}^{-1}$ . Ozone concentration in water was determined by  $\text{DO}_3$  meter. The UV–vis irradiation intensity of UV lamp was measured by diffraction grating spectrometer (Model EPP 2000, StellarNet, Oldsmar, FL, USA).

The analyses of phenol concentration were performed using the HPLC (Model 500, Viscotek, Houston, TX, USA) with  $250\text{ mm} \times 4.6\text{ mm}$  C18 column (LC-18, Supelco, Bellefonte, PA, USA) to separate the phenol and by-products of ozonation. The wavelength of UV/visible detector (Model 1706, Bio-Rad, Hercules, CA, USA) was set at 270 nm. Effluent is composed of  $\text{CH}_3\text{CN}$  and DI water ( $\text{CH}_3\text{CN}/\text{DI water} = 50/50, \text{ v/v}$ ) with flow rate controlled at  $1.0\text{ mL min}^{-1}$ . Total organic carbon (TOC) was analyzed using TOC analyzer (Model 1010, O.I. analytical, College Station, TX, USA).

## 3. Results and discussion

### 3.1. Decomposition of phenol via ozonation and photolysis ozonation in HGRPB

The decomposition efficiencies of phenol ( $\eta_{\text{phe}}$ ) in HGRPB systems of HG-OZ and HG-UV-OZ are shown in Fig. 2. No Pt/ $\gamma\text{-Al}_2\text{O}_3$  catalyst was used in these cases. The glass beads of 4 mm in diameter were packed in the RPB as packing material. Liquid volume in HGRPB is limited by the porosity of the packed bed ( $\varepsilon_B$ ). The total volume of the packed bed is  $213.88\text{ cm}^3$  with the volume of packed catalyst of  $72.05\text{ cm}^3$  and stainless wire of  $18.27\text{ cm}^3$ . This gives the free space of the packed bed of  $123.56\text{ cm}^3$ . Thus, the  $\varepsilon_B$  of HGRPB in this experiment is 57.77%. The flow rate of recycled liquid ( $Q_{\text{LR}}$ ) of the HG system is controlled at  $462\text{ mL min}^{-1}$  and the volume of phenol solution in reactor ( $V_L$ ) is 0.85 L. Hence, the turnover rate ( $\tau_T = Q_{\text{LR}}/V_L$ ) of the system is  $0.54\text{ min}^{-1}$ . For the ozonation, the applied ozone dosage per volume of liquid ( $m_{\text{A},\text{in}}$ ) and  $\eta_{\text{phe}}$  are defined as follows:

$$m_{\text{A},\text{in}} (\text{mg L}^{-1}) = Q_G \times C_{\text{AG},\text{in}} \times t \times V_L^{-1} \quad (1)$$

$$\eta_{\text{phe}} (\%) = \frac{C_{\text{BLO}} - C_{\text{BL}}}{C_{\text{BLO}}} \times 100 \quad (2)$$

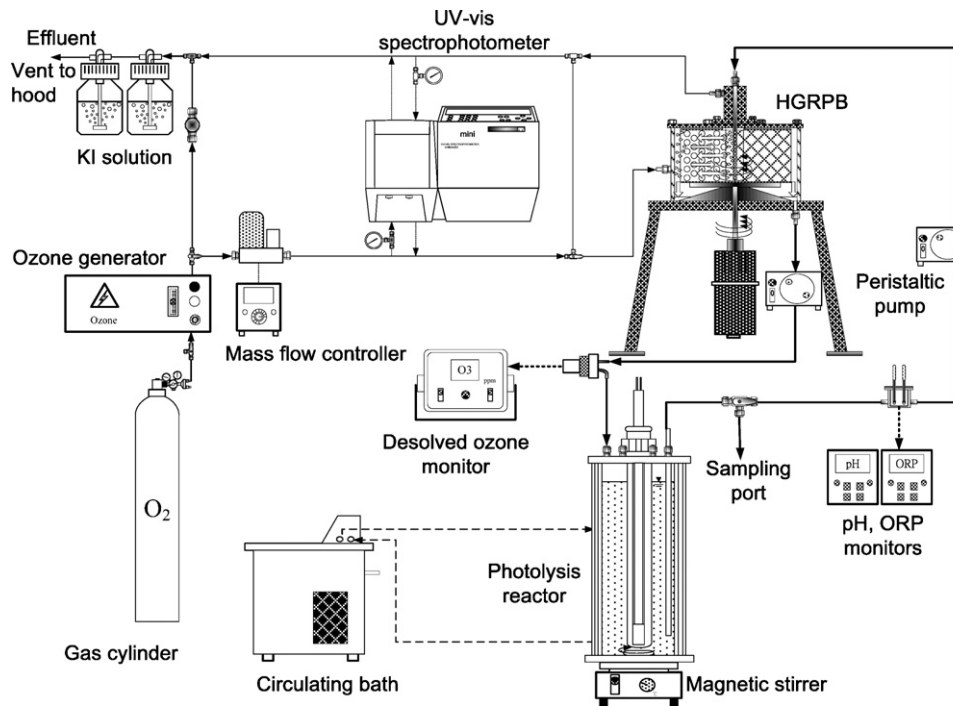


Fig. 1. Schematic diagram of high-gravity rotating packed bed (HGRPB) ozonation system.

where  $Q_G$ ,  $C_{AG,in}$  and  $V_L$  are gas flow rate, concentration of inlet ozone and volume of liquid sample, while  $C_{BLO}$  and  $C_{BL}$  are concentrations of phenol at time  $t=0$  and  $t$ .

The results show that phenol is highly reactive with  $O_3$  in the HG-OZ system. The values of  $\eta_{phe}$  for the HG-OZ and HG-UV-OZ processes are about 89% and 85% at 5 min ( $m_{A,in} = 300 \text{ mg L}^{-1}$ ), respectively. Both of them reach completely decomposition at 20 min ( $m_{A,in} = 1200 \text{ mg L}^{-1}$ ), revealing effective decomposition of phenol via the HG-OZ process. No significant reductions of phenol for the HG and HG-UV processes without ozone and catalyst were observed in the conditions studied as shown in Fig. 3. Vilaseñor et al. [2] used manganese dioxide supported on titania as catalysts and ozone as the oxidant agent for the photodegradation of phenol. The results indicate that in absence of ozone and/or catalysts, the UV does not induce a significant degradation of the phenol.

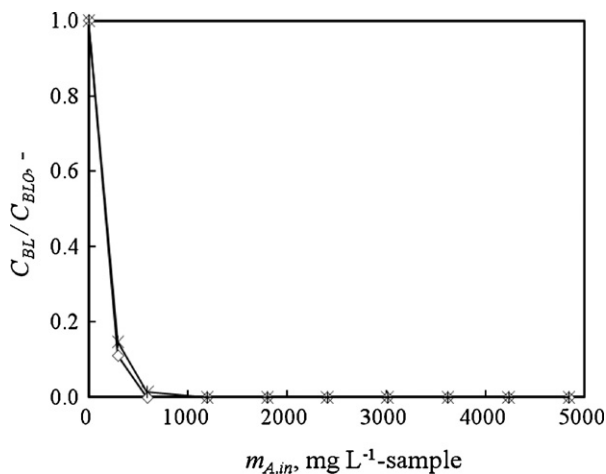


Fig. 2. Variations of  $C_{BL}/C_{BLO}$  with  $m_{A,in}$  of different AOPs in HGRPB.  $C_{BLO} = 100 \text{ mg L}^{-1}$ ,  $V_L = 1 \text{ L}$ ,  $N_r = 1500 \text{ rpm}$ ,  $T = 25^\circ \text{C}$ ,  $Q_G = 1 \text{ L min}^{-1}$ ,  $P_{UV} = 16 \text{ W}$  and  $C_{AG,in} = 60 \text{ mg L}^{-1}$  for processes with UV and ozone, respectively. ( $\diamond$ ) HG-OZ; ( $\times$ ) HG-UV-OZ.

The time variations of normalized TOC concentration ( $C_{TOC}/C_{TOC0}$ ) via HG-OZ and HG-UV-OZ are also shown in Fig. 3 along with those via HG and HG-UV. For the cases without ozone, oxygen gas was introduced to maintain the same hydraulic conditions. The value of mineralization efficiency of TOC ( $\eta_{TOC} = (C_{TOC0} - C_{TOC})/C_{TOC0}$ ) for the HG-OZ process reaches 50% at  $m_{A,in} = 2400 \text{ mg L}^{-1}$  (in 40 min) and 82% at  $m_{A,in} = 4800 \text{ mg L}^{-1}$  (in 80 min). Thus, both phenol and its by-products are highly reactive with ozone.

Combination of HG-OZ with the UV irradiation (HG-UV-OZ) can further enhance the decomposition of organic by-products. As shown in Fig. 3, at 20 min oxidation ( $m_{A,in} = 1200 \text{ mg L}^{-1}$ ),  $\eta_{TOC}$  of HG-UV-OZ is 54%, while that of HG-OZ without the UV irradiation is 24%. After 80 min oxidation ( $m_{A,in} = 4800 \text{ mg L}^{-1}$ ), the  $\eta_{TOC}$  of HG-UV-OZ is as high as 94%.

The UV-OZ is an indirect ozonation which acts on organic compounds with the radical species formed via the photolysis of  $O_3$  in

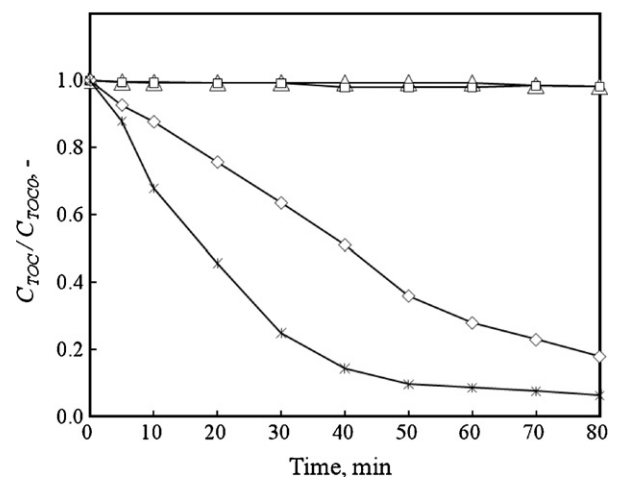


Fig. 3. Variations of  $C_{TOC}/C_{TOC0}$  with time for the mineralization of phenol via ozonation and photolysis ozonation in HGRPB. The operation conditions are the same as in Fig. 2. ( $\Delta$ ) HG; ( $\square$ ) HG-UV; ( $\diamond$ ) HG-OZ; ( $\times$ ) HG-UV-OZ.

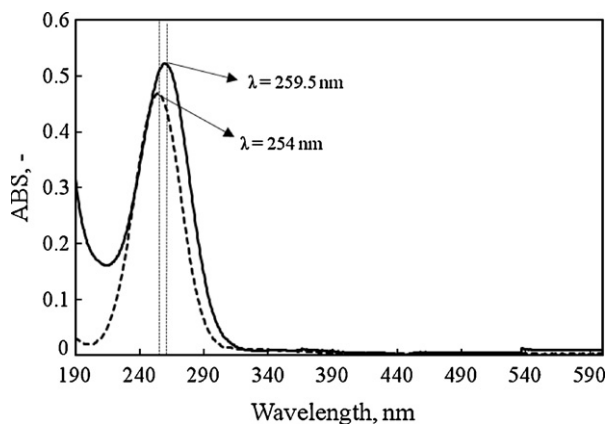


Fig. 4. Ozone absorption spectrum. (—) Dissolved ozone; (---) gaseous ozone.

water. In aqueous phase, the dissolved ozone can be decomposed directly into hydroxyl radical via the UV irradiation [15]. However, under the UV irradiation, the  $O_3$  can be also decomposed into hydrogen peroxide ( $H_2O_2$ ). The  $H_2O_2$  may be further decomposed to form hydroxyl radical via photolysis or ozonation.

The low-pressure UV lamp used in this study is a multi-wavelengths light source with three regions of UV-A (315–400 nm), UV-B (280–315 nm) and UV-C (200–280 nm) and the irradiation intensities are 3.99, 1.59 and 3.73  $W m^{-2}$ , respectively. Metering the absorption of UV irradiation in HG-UV-OZ process, UV-C region has significant absorption. The absorption spectrum of dissolved ozone and molecular ozone are shown in Fig. 4. The dissolved molecular ozone absorbs short-UV light in 190–300 nm with the maximum absorption coefficient at 259.5 nm and the gaseous ozone absorbs short-UV light in 200–300 nm with the maximum absorption coefficient at 254 nm. Furthermore, molecular phenol has obvious UV absorption below 280 nm. In HGRPB system, the photolysis was proceeding in photolysis reactor which has no gaseous ozone in it. Thus the UV-C energy was mainly adsorbed by dissolved ozone and organic compounds. Therefore, the UV-C region irradiation is absorbed by: (1) molecular ozone – enhancing the decomposition of ozone in water and generating highly reactive hydroxyl radicals and  $H_2O_2$ , (2) phenol molecule – absorbing UV-C via the aromatic ring and (3) intermediates from the decomposition of phenol – absorbing UV and reacting with ozone and hydroxyl radicals to yield other by-products.

The results of the decomposition of phenol of HG-UV using the low-pressure UV lamp indicate that the  $\eta_{phe}$  is as low as 1% during reaction time ( $t=80$  min). Thus, phenol is hard to be destructed via UV irradiation only. This then supports that in the photolysis ozonation processes, the UV energy is mainly absorbed for enhancing the decomposition of dissolved ozone and generating highly reactive hydroxyl radicals and  $H_2O_2$ .

The initial pH value of sample solution was about 7.2. In the HG-OZ process, the pH value decreased from 7.2 to 3.4 in 5 min ( $m_{A,in}=300$   $mg L^{-1}$ ) and maintained until 60 min ( $m_{A,in}=3600$   $mg L^{-1}$ ). It then increased to 7 at the end of reaction (80 min,  $m_{A,in}=4800$   $mg L^{-1}$ ). The pH value decreased because of the formation of acid intermediates such as oxalic acids and methanoic acids [6].

### 3.2. Decomposition of phenol via catalytic ozonation in HGRPB

In the present study, the  $Pt/\gamma-Al_2O_3$  and active alumina ( $\gamma-Al_2O_3$ ) of 4 mm in diameter were packed in the RPB to replace the glass bead for enhancing the ozonation efficiency of phenol. Beforehand, the possible adsorptions of phenol on the  $Pt/\gamma-Al_2O_3$  and  $\gamma-Al_2O_3$  were evaluated. The result for the case of  $\gamma-Al_2O_3$

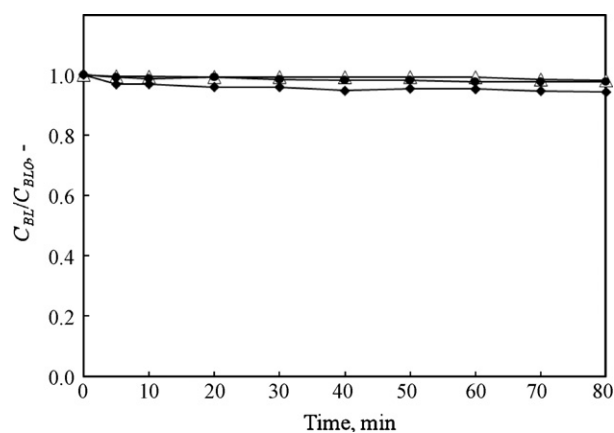


Fig. 5. Adsorption of aqueous phenol on  $Pt/\gamma-Al_2O_3$  in HGRPB systems of HG and HG-Cat. The operation conditions are the same as in Fig. 2 while the working gas is  $O_2$ . ( $\Delta$ )  $m_S=0$  g; ( $\bullet$ )  $m_S=42$  g; ( $\blacklozenge$ )  $m_S=77$  g.

reveals that  $\gamma-Al_2O_3$  dose not show any affinity for the adsorption of phenol at the conditions of  $Q_G=1$   $L min^{-1}$ ,  $Q_{LR}=100$   $mL min^{-1}$  and  $N_r=1500$  rpm. Roostaei and Tezel [16] indicated that  $\gamma-Al_2O_3$  is a porous form of aluminum oxide ( $Al_2O_3 \cdot nH_2O$ ) with a high surface area and strongly polar surface. It has both acidic and basic characteristics. The affinity of  $\gamma-Al_2O_3$  for water molecules is higher than that for phenol molecules, exhibiting negligible adsorption of phenol. Fig. 5 shows the results adsorption of phenol on  $Pt/\gamma-Al_2O_3$ . With mass of  $Pt/\gamma-Al_2O_3$   $m_S=42$  g, the adsorption of phenol is negligible. However, as  $m_S$  increases to 77 g, the  $\eta_{phe}$  can reach to 6%. Thus, the noble metal Pt on  $\gamma-Al_2O_3$  surface acting as active sites has the ability to adsorb phenol.

The decomposition of phenol in the HG-Cat-OZ is shown in Fig. 6. Similarly to the HG-OZ and HG-UV-OZ, phenol can be reduced rapidly and completely decomposed at  $m_{A,in}=1000$   $mg L^{-1}$ . No significant enhancement of  $\eta_{phe}$  is achieved using  $Pt/\gamma-Al_2O_3$  along with the HG-OZ process.

Fig. 7 presents the decomposition of TOC in the HG-Cat-OZ process with and without catalysts  $Pt/\gamma-Al_2O_3$  and  $\gamma-Al_2O_3$ . A comparison with the results of HG-OZ indicates that phenol and intermediates are decomposed rapidly because of the presence of  $Pt/\gamma-Al_2O_3$  which promotes the dissolved  $O_3$  to form high reactive  $\bullet OH$  radicals. For the case without catalyst, glass beads were used. The values of  $\eta_{TOC}$  for HG-Cat-OZ process with  $m_S=42$  g are 56% and 87% at  $m_{A,in}=1200$  and 4800  $mg L^{-1}$ , corresponding to 30 and

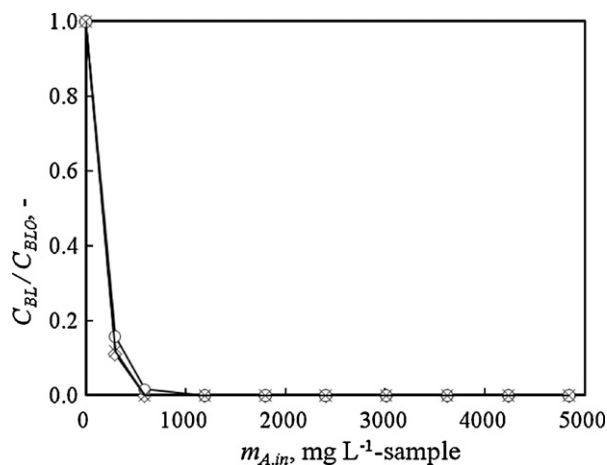
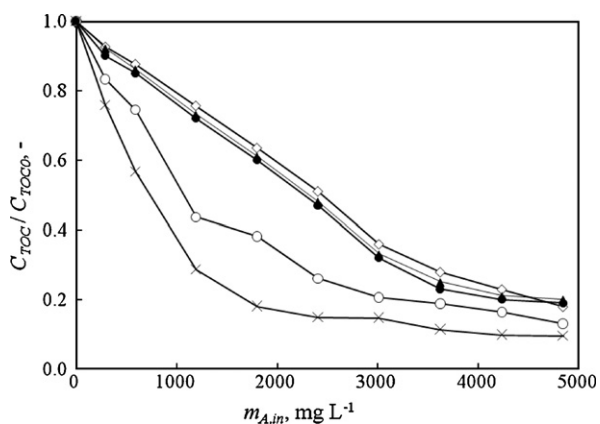


Fig. 6. Variation of  $C_{BL}/C_{BLO}$  with  $m_{A,in}$  for HG-Cat-OZ process at various  $m_S$  of  $Pt/\gamma-Al_2O_3$ . The operation conditions are the same as in Fig. 2. ( $\diamond$ )  $m_S=0$  g; ( $\circ$ )  $m_S=42$  g; ( $\times$ )  $m_S=77$  g.



**Fig. 7.** Variations of  $C_{\text{TOC}}/C_{\text{TOC}0}$  with  $m_{A,\text{in}}$  for the mineralization of phenol via HG-Cat-OZ processes. The operation conditions are the same as in Fig. 2. ( $\diamond$ )  $m_S = 0$  g; ( $\blacktriangle$ )  $\gamma\text{-Al}_2\text{O}_3$ ,  $m_S = 40$  g; ( $\bullet$ )  $\gamma\text{-Al}_2\text{O}_3$ ,  $m_S = 71$  g; ( $\circ$ ) Pt/ $\gamma\text{-Al}_2\text{O}_3$ ,  $m_S = 42$  g; ( $\times$ ) Pt/ $\gamma\text{-Al}_2\text{O}_3$ ,  $m_S = 77$  g.

80 min, respectively. By increasing the catalyst mass to 77 g, the  $\eta_{\text{TOC}}$  reaches 71% and 90% at  $m_{A,\text{in}} = 1200$  and 4800  $\text{mg L}^{-1}$ , corresponding to 30 and 80 min, respectively. The  $\eta_{\text{TOC}}$  increases with  $m_S$  because more active sites are available to adsorb  $\text{O}_3$  to form  $\bullet\text{OH}$  radical to destroy organic compounds.

The Pt contented catalyst is effective for the decomposition of  $\text{O}_3$  in aqueous phase. Lin et al. [10] used catalysts with noble metal supported on metal oxide surface to decompose aqueous ozone. Their results showed that the catalysts with noble metals supported on  $\text{Al}_2\text{O}_3$  have high activities for the decomposition of aqueous ozone. Thus, Pt/ $\text{Al}_2\text{O}_3$  catalyst was chosen for further investigation in the present study. The average rate of the decomposition of aqueous ozone on Pt/ $\text{Al}_2\text{O}_3$  is  $0.24 \text{ mg}_{(\text{O}_3)} \text{ min}^{-1} \text{ g}_{(\text{cat.})}^{-1}$  (or  $1453.78 \text{ mg}_{(\text{O}_3)} \text{ min}^{-1} \text{ g}_{(\text{metal})}^{-1}$ ). Their results further indicated that platinum has the best catalytic activity among the noble metals examined. The Pt on the Dash 220N surface assists the generation of  $\bullet\text{OH}$  radicals. The organic molecules (phenol and intermediates) are adsorbed on the Dash 220N surface and oxidized via an electron-transfer reaction. Then the organic radical species are desorbed from the Dash 220N and oxidized by  $\bullet\text{OH}$  radical or  $\text{O}_3$ .

A comparison with the results of HG-OZ ( $m_S = 0$  g) process indicates that the addition of  $\gamma\text{-Al}_2\text{O}_3$  has no significant enhancement of decomposition of TOC. Although  $\gamma\text{-Al}_2\text{O}_3$  has good performance as a catalyst support, but the low organic adsorption ability makes it in-effective on catalytic ozonation. Thus, the results reveal that

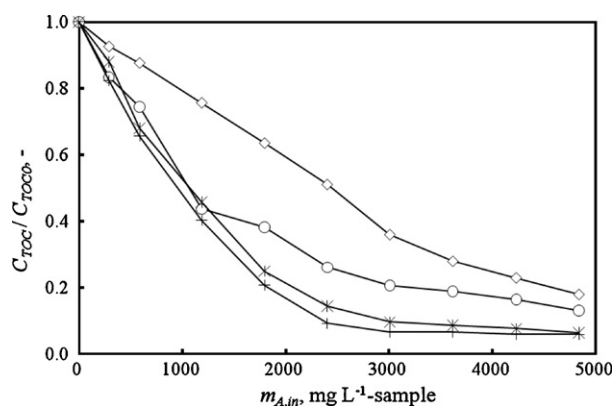


**Fig. 8.** Variations of  $C_{\text{TOC}}/C_{\text{TOC}0}$  with  $m_{A,\text{in}}$  for the mineralization of phenol using different ozone-assisted AOPs in HGRPB. The operation conditions are the same as in Fig. 2.  $P_{\text{UV}} = 16$  W for processes with UV. ( $\diamond$ ) HG-OZ; ( $\circ$ ) HG-Cat-OZ,  $m_S = 42$  g; ( $\blacktimes$ ) HG-UV-OZ; (+) HG-Cat-UV-OZ,  $m_S = 42$  g.

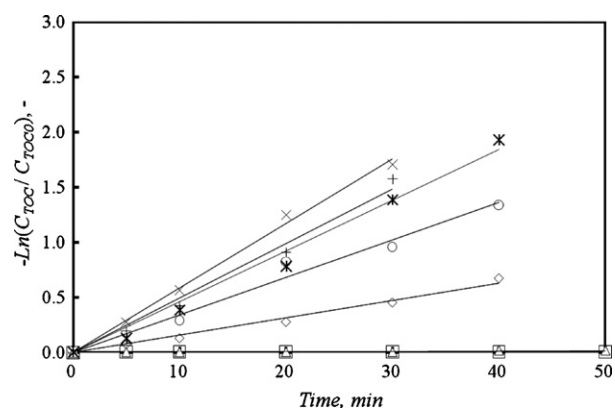


**Fig. 9.** Plots of natural logarithm of the relative organic concentration vs. time for different HGRPB systems. The operation conditions are the same as in Fig. 2. ( $\times$ ) HG-Cat-OZ,  $m_S = 77$  g; (+) HG-Cat-UV-OZ,  $m_S = 42$  g; ( $\blacktimes$ ) HG-UV-OZ; ( $\circ$ ) HG-Cat-OZ,  $m_S = 42$  g; ( $\diamond$ ) HG-OZ; ( $\square$ ) HG-UV; ( $\triangle$ ) HG.

**Table 1**

Pseudo-first order kinetic rate constants of decomposition of TOC for different HG processes.

Process	$k$ ( $\text{min}^{-1}$ )
HG- $\text{O}_2$	0.0003
HG-UV	0.0003
HG-OZ	0.0158
HG-Pt-OZ ( $m_S = 42$ g)	0.0340
HG-UV-OZ	0.0460
HG-Pt-UV-OZ ( $m_S = 42$ g)	0.0495
HG-Pt-OZ ( $m_S = 77$ g)	0.0585

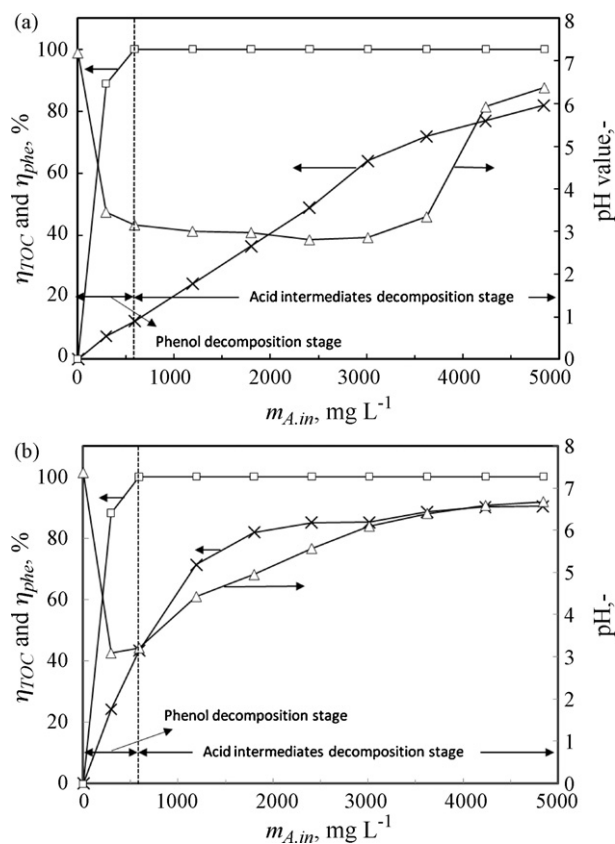


**Fig. 10.** The relationships of  $\eta_{\text{TOC}}$ ,  $\eta_{\text{phe}}$  and pH value with  $m_{A,\text{in}}$ . (a) HG-OZ and (b) HG-Cat-UV-OZ. The operation conditions are the same as in Fig. 2.  $P_{\text{UV}} = 16$  W for HG-Cat-UV-OZ. ( $\square$ )  $\eta_{\text{phe}}$ ; ( $\triangle$ ) pH value; ( $\times$ )  $\eta_{\text{TOC}}$ .

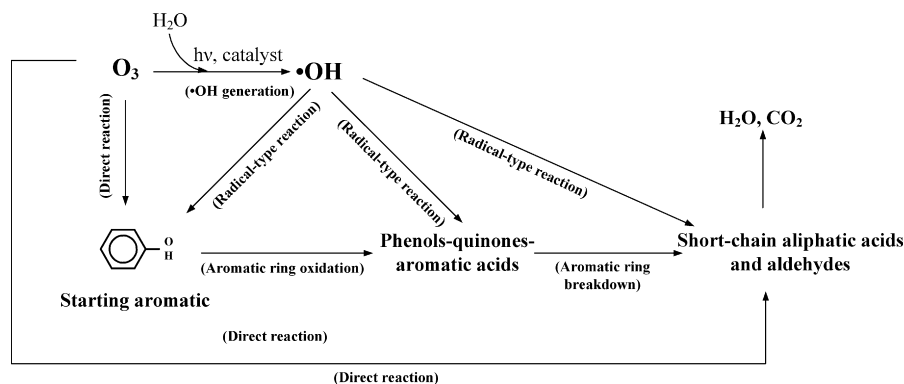


Fig. 11. Simplified scheme illustrating the possible mechanism for the ozonation of phenol with UV and catalyst.

without Pt on  $\gamma$ - $\text{Al}_2\text{O}_3$  surface in HG-OZ system, the phenol is decomposed via direct ozonation. Lin et al. [8] also indicated that the average rate of the decomposition of aqueous ozone on  $\text{Al}_2\text{O}_3$  is as low as  $0.01 \text{ mg}_{(\text{O}_3)} \text{ min}^{-1} \text{ g}_{(\text{cat.})}^{-1}$  while those on active carbon and Pt/ $\text{Al}_2\text{O}_3$  are as high as 0.25 and  $0.24 \text{ mg}_{(\text{O}_3)} \text{ min}^{-1} \text{ g}_{(\text{cat.})}^{-1}$ , respectively. All these results indicated that the  $\text{Al}_2\text{O}_3$  has very low or no activity on catalytic ozonation.

### 3.3. Phenol decomposition via combination of photolysis and catalytic ozonation in HGRPB

Combining UV irradiation in the HG-Cat-OZ process (denoted as HG-Cat-UV-OZ) can further enhance the decomposition of phenol as shown in Fig. 8. At the same conditions with Pt/ $\gamma$ - $\text{Al}_2\text{O}_3$  packing mass  $m_S = 42 \text{ g}$  and  $m_{A,in} = 2404 \text{ mg L}^{-1}$  (40 min oxidation), the  $\eta_{\text{TOC}}$  of HG-Cat-UV-OZ is 91%, while that of HG-Cat-OZ without UV irradiation is 74%. The values of  $\eta_{\text{TOC}}$  of HG-Cat-UV-OZ and HG-Cat-OZ at  $m_{A,in} = 4800 \text{ mg L}^{-1}$  (80 min) are 94% and 87%. The combination of UV irradiation in HG-Cat-OZ can reach a high decomposition efficiency of TOC at a lower  $m_{A,in}$  or shorter ozonation time.

### 3.4. Comparison of pseudo-first order kinetic rate constants of decomposition TOC in different HGRPB systems

The decomposition efficiency of TOC with ozone in HG processes is affected by rotating speed, ozone gas flow rate, temperature, catalyst packing mass and UV irradiation intensity. Fig. 9 shows the time variation of  $-\ln(C_{\text{TOC}}/C_{\text{TOC}0})$  for different HG processes at fixed conditions of  $C_{\text{BL}0}$ ,  $N_r$ ,  $T$  and  $Q_G$ . The value of the pseudo-first order kinetic rate constant ( $k$ ) was obtained by fitting the experimental kinetic data in Fig. 9 and listed in Table 1. The HG-Pt-OZ with  $m_S = 77 \text{ g}$  exhibiting the highest  $k$  value of  $0.0585 \text{ min}^{-1}$ , which is higher than the HG-Cat-UV-OZ ( $m_S = 42$ ) of  $0.0495 \text{ min}^{-1}$  and four times higher than the HG-OZ of  $0.0158 \text{ min}^{-1}$ . For the sole photolysis of phenol, the  $k$  is very low with value of  $0.003 \text{ min}^{-1}$  only. The  $k$  value of HG-UV-OZ is 0.0460. Thus, the introduction of UV and Pt/ $\gamma$ - $\text{Al}_2\text{O}_3$  catalyst in the HG-OZ process greatly improves the decomposition efficiency of TOC in ozonation.

### 3.5. Decomposition mechanism

The mineralization of phenol can be classified into phenol decomposition stage and acid intermediates decomposition stage. Fig. 10a and b shows the relationships of  $\eta_{\text{TOC}}$ ,  $\eta_{\text{pHe}}$  and pH value with  $m_{A,in}$  in the HG-OZ and HG-Cat-UV-OZ processes, respectively. In the phenol decomposition stage ( $m_{A,in} = 0\text{--}600 \text{ mg L}^{-1}$  or time = 0–10 min), molecular phenol is firstly decomposed to acid intermediates, resulting in the decrease of pH value. While in the

acid intermediates decomposition stage ( $m_{A,in} = 600\text{--}4800 \text{ mg L}^{-1}$  or time = 10–80 min), the concentration of TOC decreases with  $m_{A,in}$ , reflecting the further decomposition of acid intermediates and resulting in the increase of pH value to neutral. The rising of pH value in turn results in further decomposition of organic acids. In the ozone assisted HG systems, the variation of pH value can provide the information for realizing the progress of the decomposition of phenol. For the HG-UV-OZ, HG-Pt-OZ and HG-Pt-UV-OZ processes, the pH value decreases from 7.2 to 3–4 in 5 min and then increases to 5–7 at the end of the reaction. The rising of pH value is faster for the system with higher mineralization ability. Thus, the HG-Pt-UV-OZ process reaches the final pH value faster than the HG-OZ process.

A simplified scheme of the decomposition pathways of phenol for the catalytic ozonation with UV is shown in Fig. 11. Both the phenol and intermediates are attacked by  $\text{O}_3$  and  $\bullet\text{OH}$  radical. The initial attack of oxidants on phenol during ozonation is via the electrophilic addition to form aromatic acids. Then the aromatic rings are broken down by  $\text{O}_3$  and  $\bullet\text{OH}$  radical to form short-chain organic acids such as oxalic acid, glyoxalic acid and formic acid. These short-chain organic acids are further decomposed to  $\text{CO}_2$  and  $\text{H}_2\text{O}$  eventually.

## 4. Conclusions

The decompositions of phenol via HG-OZ, HG-UV-OZ, HG-Pt-OZ and HG-Pt-UV-OZ are investigated in this study. Several conclusions can be drawn as follows:

- (1) The introduction of UV irradiation in the HG-OZ can enhance both the decomposition and mineralization of phenol significantly. The molecular ozone absorbs UV-C energy resulting in self-decomposition to form high active radicals. The value of mineralization efficiency  $\eta_{\text{TOC}}$  employing the HG-UV-OZ process is 94% at applied ozone dosage per volume of liquid sample  $m_{A,in} = 4800 \text{ mg L}^{-1}$  or reaction time = 80 min.
- (2) Packing Pt/ $\gamma$ - $\text{Al}_2\text{O}_3$  catalyst (Dash 220N) in the HG-OZ process can also effectively enhance the decompositions of phenol and intermediates under the experimental conditions of this study. The  $\eta_{\text{TOC}}$  of phenol increases from 82% of HG-OZ to 90% of HG-Pt-OZ ( $m_S = 77 \text{ g}$ ) at  $m_{A,in} = 4800 \text{ mg L}^{-1}$  or reaction time = 80 min because of the formation of  $\bullet\text{OH}$  radicals. Packing  $\gamma$ - $\text{Al}_2\text{O}_3$  in RPB has no significant catalytic efficiency for ozonation.
- (3) The use of UV irradiation in HG-Pt-OZ process further significantly enhances both the decomposition and mineralization efficiencies of phenol. At  $m_{A,in} = 4800 \text{ mg L}^{-1}$ ,  $m_S = 42 \text{ g}$  and power of UV  $P_{\text{UV}} = 16 \text{ W}$ , the  $\eta_{\text{TOC}}$  is as high as 94%. The HG-UV-OZ process mainly absorbs UV-C ( $\lambda = 200\text{--}280 \text{ nm}$ ) energy

to decompose ozone to form high active radicals. The photolysis of phenol via UV irradiation (HG-UV) only is negligible.

- (4) The values of pseudo-first order kinetic rate constants  $k$  of decomposition of TOC for the HG-Cat-OZ with  $m_S$  of 42 g, HG-Cat-UV-OZ with  $m_S$  of 42 g and HG-Cat-OZ with  $m_S$  of 77 g are 0.034, 0.0495 and 0.0585  $\text{min}^{-1}$ , respectively. The introduction of UV greatly increases the value of  $k$  of the ozonation process. However, the increase of the amount of catalyst can also provide the enhancement effect, increasing the value of  $k$  of HG-OZ process.

#### Nomenclature and units

AOPs	advanced oxidation processes
$a$	specific area of gas-liquid interface per unit volume of contactor or packed bed ( $\text{m}^2 \text{m}^{-3}$ )
$C$	concentration ( $\text{mg L}^{-1}$ )
$C_{AG,in}$	$C$ of feed $\text{O}_3$ ( $\text{mg L}^{-1}$ )
$C_{BL}$	$C$ of phenol ( $\text{mg L}^{-1}$ )
$C_{BLO}$	initial $C$ of phenol ( $\text{mg L}^{-1}$ )
$C_{TOC}, C_{TOCO}$	$C$ of TOC at time = $t$ and 0 ( $\text{mg L}^{-1}$ )
HGRPB, HG or Hige	high-gravity rotating packed bed
HG-Cat-OZ	catalytic HG-OZ
HG-Cat-UV-OZ	catalytic HG-UV-OZ
HG-OZ	HGRPB-ozonation
HG-UV	ultra violet HG
HG-UV-OZ	ultra violet HG-OZ
HRT	hydraulic retention time (s)
$k_{LA}$	physical liquid-phase mass transfer coefficient of ozone ( $\text{m s}^{-1}$ )
$m_{A,in}$	applied dosage of ozone per volume of sample ( $\text{mg L}^{-1}$ )
$m_S$	mass of catalyst (g)
$N_r$	rotating speed of HGRPB (rpm)
$P_{UV}$	power of light source of UV (W)
$Q_G$	flow rate of feed $\text{O}_3$ ( $\text{L min}^{-1}$ )
$Q_{LR}$	flow rate of recycled liquid ( $\text{L min}^{-1}$ )
$r_T$	turnover rate of semi-batch system ( $\text{min}^{-1}$ )
$T$	temperature ( $^{\circ}\text{C}$ )
TOC	total organic carbon
$t$	reaction time (min)
$V_L$	sample volume (L)
$\varepsilon_B$	porosity of packed bed

$\eta_{phe}$  decomposition efficiency of phenol,  $1 - C_{BL}/C_{BLO}$   
 $\eta_{TOC}$  mineralization efficiency of TOC,  $1 - C_{TOC}/C_{TOCO}$

#### Acknowledgment

The authors would like to thank the National Science Council of Taiwan for the financial support of the work (NSC 93-2211-E267-005).

#### References

- [1] B. Legube, N.K. Vel Leitner, Catalytic ozonation: a promising advanced oxidation technology for water treatment, *Catal. Today* 53 (1999) 61–72.
- [2] J. Villaseñor, P. Reyes, G. Pecchi, Catalytic and photocatalytic ozonation of phenol on  $\text{MnO}_2$  supported catalysts, *Catal. Today* 76 (2002) 121–131.
- [3] Y.H. Chen, C.Y. Chiu, C.Y. Chang, Y.H. Huang, Y.H. Yu, P.C. Chiang, J.L. Shie, C.S. Chiou, Modeling ozonation process with pollutant in a rotating packed bed, *Ind. Eng. Chem. Res.* 44 (2005) 21–29.
- [4] Y.H. Chen, C.Y. Chang, C.C. Chen, C.Y. Chiu, Kinetics of ozonation of 2-mercaptothiazoline in an electroplating solution combined with UV radiation, *Ind. Eng. Chem. Res.* 45 (2006) 4936–4943.
- [5] W.J. Huang, Y.L. Cheng, B.L. Cheng, Effect of water quality on destruction of odor causing substances during ozonation processes, *J. Environ. Eng. Manage.* 17 (2007) 257–265.
- [6] Y.C. Hsu, J.H. Chen, H.C. Yang, Calcium enhanced COD removal for the ozonation of phenol solution, *Water Res.* 41 (2007) 71–78.
- [7] P.K.A. Hong, Y. Huang, C.F. Lin, A.Y.C. Lin, Pressure-assisted  $\text{O}_3/\text{H}_2\text{O}_2$  process for degradation of MTBE, *J. Environ. Eng. Manage.* 18 (2008) 239–247.
- [8] M.C. Wu, N.A. Kellyb, Clean-air catalyst system for on-road applications. I. Evaluation of potential catalysts, *Appl. Catal. B* 18 (1998) 79–91.
- [9] K.C. Cho, K.C. Hwang, T. Sano, K. Takeuchi, S. Matsuzawa, Photocatalytic performance of Pt-loaded  $\text{TiO}_2$  in the decomposition of gaseous ozone, *J. Photochem. Photobiol. A* 161 (2004) 155–161.
- [10] J. Lin, A. Kawai, T. Nakajima, Effective catalysts for decomposition of aqueous ozone, *Appl. Catal. B* 39 (2002) 157–165.
- [11] C.C. Lin, W.T. Liu, Ozone oxidation in a rotating packed bed, *J. Chem. Technol. Biotechnol.* 78 (2003) 138–141.
- [12] C. Ramshaw, R.H. Mallinson, Mass Transfer Process, U.S. Patent 4,283,225 (1981).
- [13] C.C. Chang, C.Y. Chiu, C.Y. Chang, C.F. Chang, Y.H. Chen, D.R. Ji, Y.H. Yu, P.C. Chiang, Combined photolysis and catalytic ozonation of dimethyl phthalate in a high-gravity rotating packed bed, *J. Hazard. Mater.* 161 (2009) 287–293.
- [14] L.H. Nowell, J. Hoign, Interaction of iron (II) and other transition metals with aqueous ozone, in: Proceedings of the 8th Ozone World Congress, IOA, Zurich, Switzerland, 1988, pp. E80–E95.
- [15] G.R. Peyton, W.H. Glaze, Destruction pollutants in water with ozone in combination with ultraviolet radiation. 3. Photolysis of aqueous ozone, *Environ. Sci. Technol.* 22 (1988) 761–767.
- [16] N. Roostaei, F.H. Tezel, Removal of phenol from aqueous solutions by adsorption, *J. Environ. Manage.* 70 (2004) 157–164.